Direct test of the Gaussian auxiliary field ansatz in nonconserved order parameter phase ordering dynamics

Chuck Yeung*

School of Science, Pennsylvania State University at Erie, The Behrend College, Erie, Pennsylvania 16563, USA

(Received 28 December 2017; revised manuscript received 12 May 2018; published 4 June 2018)

The assumption that the local order parameter is related to an underlying spatially smooth auxiliary field, $u(\vec{r},t)$, is a common feature in theoretical approaches to non-conserved order parameter phase separation dynamics. In particular, the ansatz that $u(\vec{r},t)$ is a Gaussian random field leads to predictions for the decay of the autocorrelation function which are consistent with observations, but distinct from predictions using alternative theoretical approaches. In this paper, the auxiliary field is obtained directly from simulations of the time-dependent Ginzburg-Landau equation in two and three dimensions. The results show that $u(\vec{r},t)$ is equivalent to the distance to the nearest interface. In two dimensions, the probability distribution, $P(u)$, is well approximated as Gaussian except for small values of $u/L(t)$, where $L(t)$ is the characteristic length-scale of the patterns. The behavior of $P(u)$ in three dimensions is more complicated; the non-Gaussian region for small $u/L(t)$ is much larger than that in two dimensions but the tails of $P(u)$ begin to approach a Gaussian form at intermediate times. However, at later times, the tails of the probability distribution appear to decay faster than a Gaussian distribution.

DOI: 10.1103/PhysRevE.97.062107

I. INTRODUCTION

The most basic example of phase ordering dynamics occurs when a ferromagnetic system is quenched from a high temperature disordered phase into the two-phase regime. The resulting domain growth exhibits scaling and universality; the statistical distribution of the domains is described by a single time dependent length-scale which typically grows as a power law in time, $L(t) \sim t^{\alpha}$, and many different systems have the same growth exponent α. For ferromagnetic systems, $\alpha = 1/2$ if the order parameter is not conserved and $\alpha = 1/3$ if the order parameter is conserved [1,2].

Due to its simple description yet rich behavior, phase separation dynamics serves as a testing ground for theoretical approaches to non-equilibrium dynamics. The growth exponent α can be obtained from scaling analysis of the interfacial dynamics for the different cases. However, there has been less progress in our ability to calculate more quantitative features such as the order parameter correlation function,

$$C(\vec{r};t,t') = \langle \psi(\vec{R},t)\psi(\vec{R}+\vec{r},t')\rangle. \quad (1)$$

Here, $\psi(\vec{r},t)$ is the order parameter at position $\vec{r}$ and time t and the average is over both $\vec{R}$ and initial conditions. One reason for the limited progress is that, as shown in Fig. 1, the order parameter field is effectively spatially discontinuous when viewed at the length-scale of the domains. Therefore it is difficult to apply approximate methods directly to the order parameter field. An approach that has had some success is to assume the order parameter can be written as a nonlinear function of a spatially smooth auxiliary field $u(\vec{r},t)$ [3–9]. One can then make progress by applying approximate methods to the dynamics of the auxiliary field.

This approach was used to study non-conserved order parameter phase ordering by Ohta, Jasnow, and Kawasaki (OJK) [3]. They started with the Cahn-Allen equation describing the dynamics of the interfaces [10] and obtained an evolution equation for the auxiliary field $u(\vec{r},t)$. This field was interpreted, at least near interfaces, as the distance to the interface. After applying some approximations, u was found to obey the diffusion equation. From this one can obtain both the equal time correlation function $C(\vec{r};t,t)$ [3] and the autocorrelation function $C(0;t,t')$ [11].

Mazenko took an alternative approach by defining $u(\vec{r},t)$ as a nonlinear mapping of the local order parameter $\psi(\vec{r},t)$ [5]. He then makes the ansatz that $u(\vec{r},t)$ is a Gaussian random field. With this ansatz, a closed equation is obtained for the equal time correlation function [5], and for the autocorrelation function [6]. The ansatz of an underlying smooth Gaussian field has also been applied to other phase ordering systems [12,13] as well as for two-dimensional turbulence [14].

The OJK and Mazenko methods both reproduce the experimentally observed result that the characteristic length-scale grows as $L(t) \propto t^{1/2}$. The differences in the equal time correlation functions predicted by the two methods are subtle and both are close to simulation results [15,16]. A more sensitive test of the two approaches is to consider how the system at time t is related to the system at an earlier time t' [6,7,11,17–31]. One way to quantify this effect is through the autocorrelation function $C(t,t') = C(0;t,t')$. In the scaling regime, $C(t,t')$ should be a function only of the ratio of length-scales $y = L(t)/L(t')$. Furthermore, for $y \gg 1$, the autocorrelation function should decay as a power law in y, i.e., $C(t,t') \sim y^{-\lambda}$ [6,11,17,20].

In contrast to the equal-time correlation function, the differences in the autocorrelation exponent λ predicted by the OJK model and the Gaussian ansatz approaches are readily observable. The OJK model predicts that $\lambda = d/2$, where d is

*cyeung@psu.edu

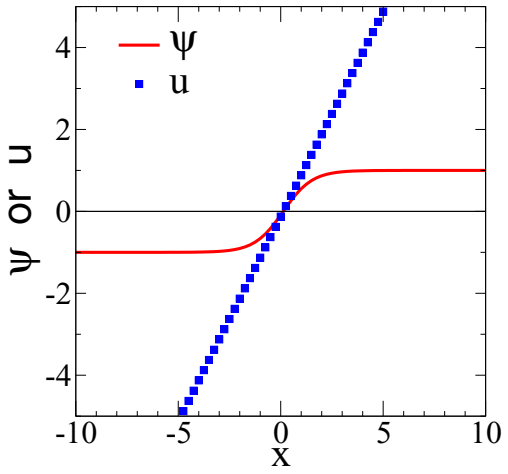

FIG. 1. At a domain boundary, the order parameter $\psi(x)$ (solid line) changes rapidly over a length-scale corresponding to the interfacial width. In the scaling regime, the characteristic domain size becomes much larger than this width, so $\psi(x)$ is effectively discontinuous on the larger length-scale. The auxiliary field $u(x)$ (filled squares) can be extracted from the order parameter field using Eq. (11) and $u(x)$ is smooth on all length-scales making approximate methods more applicable. The results in this figure are obtained from the planar interface solution for the discretized evolution equation with mesh size $\Delta x = 0.25$.

the dimension [11] while Liu and Mazenko found significantly higher values for the exponent with $\lambda = 1.2887$ for $d = 2$ and $\lambda = 1.6726$ for $d = 3$ [6,18]. The two methods coincide as $d \to \infty$ [7]. Experiments [19] and simulations [6,18,27,30] of non-conserved order parameter phase ordering give values of λ that are consistent with Liu-Mazenko but these earlier simulations were with smaller systems and limited ranges of L/L'. The values of λ obtained had large uncertainties and were susceptible to finite size and finite time effects. More recent results by Midya *et al.* [27] used finite size analysis on larger systems to decrease the uncertainty in the exponents. Their results for λ were consistent with the predictions based on the Gaussian ansatz and rule out the predictions of the OJK model.

Therefore the Mazenko-Liu analysis results in non-trivial predictions for the autocorrelation exponents that agree with simulation but are distinct from other approximate methods. Their approach relies on the ansatz that the local order parameter $\psi(\vec{r},t)$ is a nonlinear function of a Gaussian random field $u(\vec{r},t)$, but this Gaussian auxiliary field ansatz has never been tested directly. In this paper, I extract the auxiliary field $u(\vec{r},t)$ directly from simulations of the time-dependent Ginzburg-Landau equation in two and three dimensions.

In two dimensions, I find that the probability distribution, $P(u)$ for the auxiliary field displays excellent collapse, and $P(u)$, is approximately Gaussian except for a small region around $u/L(t) = 0$ implying that the Mazenko-Liu analysis is applicable in two dimensions. In three dimensions, the non-Gaussian region of $P(u)$ around small $u/L(t)$ is much larger. The tails of the probability distribution approaches a Gaussian form at intermediate times. However, at later times there appears to be a transition to a faster decay at the tails of the probability distribution function.

I also show that $u(\vec{r},t)$ is the equivalent to the distance from $\vec{r}$ to the closest interface. This equivalence is significant since in most systems, one cannot extract an auxiliary field at a point $\vec{r}$ from the state of the system near that point. On the other hand, it is always possible to define the distance to the closest interface in any model of phase ordering dynamics, therefore arguments using an auxiliary field is applicable even for those systems where one cannot extract the auxiliary field in a straightforward manner.

II. MAPPING THE ORDER PARAMETER TO THE AUXILIARY FIELD

Phase ordering dynamics following a quench to zero temperature can be described by the time-dependent Ginzburg-Landau (TDGL) equation

$$\frac{1}{\Gamma}\frac{\partial \psi}{\partial t} = -\frac{\delta F[\psi]}{\delta \psi}, \tag{2}$$

where Γ is the mobility. The Ginzburg-Landau free energy functional, F, has the form

$$F[\psi(\vec{r},t)] = \int d\vec{r}\left(V(\psi) + \frac{\xi^2}{2}|\vec{\nabla}\psi|^2\right), \tag{3}$$

where $V(\psi)$ is a symmetric double well potential with minima at $\psi = \pm\psi_{eq}$ and ξ is the interfacial width. The TDGL equation is assumed to have a time independent planar interface solution, $\psi(x) = f(x)$, where $f(x)$ is an odd function of x with $f(x) \to \pm\psi_{eq}$ as $x \to \pm\infty$. A smooth auxiliary field, $u(\vec{r},t)$, is defined by inverting this relation: $u(\vec{r},t) = f^{-1}(\psi(\vec{r},t))$ where f^{-1} is the inverse function of f. This implies that, near interfaces, $u(\vec{r},t)$ is the displacement to the interface. Making the ansatz that $u(\vec{r},t)$ is a Gaussian random field gives a closed expression for the order parameter correlation function $C(\vec{r};t)$ [5]

$$\frac{1}{2\Gamma\xi^2}\frac{\partial C}{\partial t} = \nabla^2 C + \frac{2\psi_{eq}^2}{\pi\langle u^2\rangle}\tan\left(\frac{\pi C}{2\psi_{eq}^2}\right), \tag{4}$$

where $\langle u^2\rangle = \langle u(\vec{r},t)^2\rangle$. Note that Mazenko defined the auxiliary field as $m(\vec{r},t) = u(\vec{r},t)/\sqrt{2}$ so Eq. (4) is slightly different from the equivalent expression in Ref. [5]. A similar closed expression can be obtained for the autocorrelation function, $C(t,t')$ [6].

Analysis of the scaling form of Eq. (4) for $x = r/L(t) \gg 1$ gives $C(r;t) \propto x^{d-\pi/2\mu}e^{-\mu x^2/2}$ [5]. The nonlinear eigenvalue, μ, is defined by the relation $\langle u^2\rangle = 4\mu t/\pi$ and is determined by numerically solving the scaling form of Eq. (4). The eigenvalue is found to be $\mu = 1.104$ for $d = 2$ and $\mu = 0.5917$ for $d = 3$. A similar analysis for the two-time correlation function gives the autocorrelation exponent as $\gamma = d - \pi/4\mu$ [6,7].

In this paper, $V(\psi)$ is chosen to be

$$V(\psi) = -\frac{\psi^2}{2} + \frac{\psi^4}{4}, \tag{5}$$

so that $\psi_{eq} = 1$. In dimensionless form, the time-dependent Ginzburg-Landau equation becomes

$$\frac{\partial \psi}{\partial t} = \psi - \psi^3 + \nabla^2\psi. \tag{6}$$

This equation has a time-independent planar interface solution

$$\psi(x) = \tanh\left(\frac{x}{\sqrt{2}}\right), \tag{7}$$

where the x is the displacement from the interface. Inverting this relation gives the mapping from ψ to the auxiliary field as

$$u_o(\psi) = \frac{1}{\sqrt{2}} \ln\left(\frac{1+\psi}{1-\psi}\right). \tag{8}$$

Note that $\psi(x)$ converges to its equilibrium values of ± 1 exponentially in x with a decay length of $\ell_o = 1/\sqrt{2}$. Therefore ψ is very close to its equilibrium values except very near the interface.

Space must be discretized in order to integrate the TDGL equation numerically. This leads to a Δx dependent modification of the mapping from $\psi \to u$. Linearizing Eq. (6) near $\psi = \pm 1$ shows that the decay length becomes $\ell = \alpha_{\Delta x}\ell_o$ where $\alpha_{\Delta x}$ is given by

$$\alpha_{\Delta x} = -\frac{\sqrt{2}\Delta x}{\ln(1 - \Delta x\sqrt{2 + (\Delta x)^2} + (\Delta x)^2)}. \tag{9}$$

Notice that $\alpha_{\Delta x} \to 1$ as $\Delta x \to 0$ as expected. To take the finite mesh size into account, the mapping to the auxiliary field is modified to be $u(\psi) = \alpha_{\Delta x} u_o(\psi)$. For the mesh size, $\Delta x = 1$, used for most of this work, $\alpha_{\Delta x} = 1.074$.

There is further issue that must be taken into account in order to extract u from ψ. The mapping $u_o(\psi)$ is very sensitive to how close ψ is to its equilibrium values. Therefore, except for near interfaces, it is necessary to know ψ to many digits of precision to determine u. To avoid this, the order parameter is stored in the simulation as the difference from its equilibrium values; $\phi_+ = \psi - 1$ if $\psi \geqslant 0$, and $\phi_- = \psi + 1$ if $\psi < 0$. In terms of ϕ_+, the TDGL equation [Eq. (6)] becomes

$$\frac{\partial \phi_+}{\partial t} = -2\phi_+ - 3\phi_+^2 - \phi_+^3 + \nabla^2\phi_+ \tag{10}$$

with a similar expression for $\partial\phi_-/\partial t$. Since ϕ_+ and ϕ_- both approach zero in the bulk, one can store the order parameter array in terms of $\phi_\pm$ as floating point numbers with standard precision and still extract u from $\phi_\pm$.

To test this mapping, I numerically solved the TDGL [Eq. (6)] to find the time-independent planar interface solution for $\Delta x = 0.25$, $\Delta x = 0.5$, and $\Delta x = 1.0$. In one dimension, u should be exactly equal to the displacement, x. I applied the mapping $u(\psi) = \alpha_{\Delta x} u_o(\psi)$ to the planar interface solution and found that, away from the interface, u grows at the same rate as x but is shifted from x by a constant amount. To adjust for this, a compensating shift in the mapping from ψ to u is introduced. This shift must vanish at $u = 0$ and be constant at larger distances. The final mapping used in the simulations is

$$u(\psi) = \begin{cases} \alpha_{\Delta x} u_o(\psi) - \frac{(\Delta x)^2}{5} & \text{if } u_o(\psi) \geqslant 3, \\ \alpha_{\Delta x} u_o(\psi) - \frac{u_o(\psi)(\Delta x)^2}{15} & \text{if } -3 < u_o(\psi) < 3, \\ \alpha_{\Delta x} u_o(\psi) + \frac{(\Delta x)^2}{5} & \text{if } u_o(\psi) \leqslant -3. \end{cases} \tag{11}$$

Here, $u_o(\psi)$ is the continuum limit mapping given in Eq. (8). The form of the shift and the cutoff for the constant shift at $|u| = 3$ were chosen empirically. This mapping was found to produce $u \approx x$ for all three values of Δx used. The mapping from ψ to u is shown in Fig. 1 for a planar interface with mesh size $\Delta x = 0.25$.

III. RESULTS

The time-dependent Ginzburg-Landau equation [Eq. (6)] was numerically integrated in two and three dimensions starting with random (spatially uncorrelated) initial conditions. The mesh-size used was $\Delta x = 1.0$ and the time-step was $\Delta t = 0.1$. However, some results were obtained for smaller Δx and Δt to check for mesh-size and time-step effects. In two dimensions, most of the simulations were performed for systems of size 16384^2 up to time $t = 12800$. The results were averaged over 12 initial conditions. Results using smaller systems of size 8192^2 showed no finite size effects. In three dimensions, simulations were performed for systems of size 1024^3 (25 initial conditions) to $t = 1600$. Simulations were also performed for smaller systems of size 512^3 and 256^3 to check for finite size effects. The results given below are from the largest two-dimensional (2D) and three-dimensional (3D) systems unless otherwise noted. All uncertainties quoted are based on run to run variations. Note that system sizes used here are substantially larger than the largest systems used by Midya *et al.* [27] for their finite size analysis of the autocorrelation function (1024^2 in 2D and 400^3 in 3D) or the largest 3D integration of the TDGL (700^3) by Brown and Rikvold [32].

The auxiliary field u must be equivalent to the displacement from the interface in one dimension but, except for very close to interfaces, there is no *a priori* reason that u must be this distance in higher dimensions. To check if this equivalence still holds in two and three dimensions, I determine the signed distance, $D(\vec{r},t)$, from each lattice point $\vec{r}$ to the closest interface. $D(\vec{r},t)$ is defined as positive if $\psi(\vec{r},t)$ is positive and negative otherwise.

Figure 2 shows the probability distributions $P(D)$ of D, and $P(u)$ of u for 3D systems of size 1024^3 at $t = 800$. The two distributions coincide except for a small region near $u = D = 0$, where $P(D)$ has a dip relative to $P(u)$. This difference is expected since the calculation of D near interfaces will be most affected by the finite mesh-size. Similar results were obtained for the probability distributions of u and D at different times and in two dimensions. This demonstrates that $u(\vec{r},t)$ can be interpreted as the closest distance to the interface even in two and three dimensions.

The equivalence between u and D is significant because it is not possible to define an auxiliary field from the local state of the system in most models of phase separation dynamics. For example, in a quench of the kinetic Ising model to zero temperature, the spins are either all up or all down except at the domain interfaces. One cannot extract an auxiliary field at a particular position $\vec{r}$ just from the state of the spins in the neighborhood of that position. This is true even for a standard numerical integration of the TDGL equation. To within numerical precision, the value of the order parameter $\psi(\vec{r},t)$ will reach its bulk equilibrium values except for very near interfaces and, hence, the value of u extracted from ψ will also saturate at its bulk values except for very near interfaces.

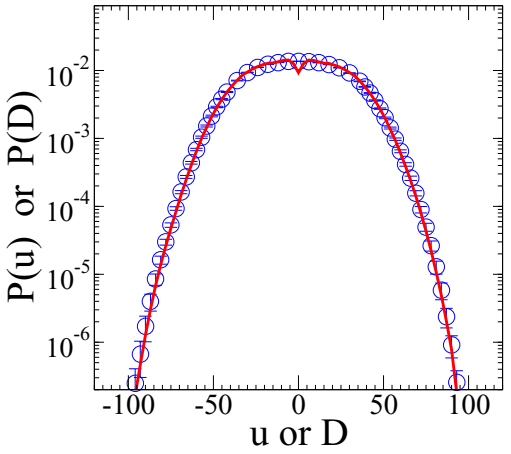

FIG. 2. Probability distribution for the auxiliary field u (open circles), and for the closest distance to interface D (solid line). The results are for three-dimensional systems of size 1024^3 at $t = 800$. The two distributions coincide except for near interfaces where the effect of the mesh-size is apparent. Similar agreement between $P(u)$ and $P(D)$ is found in two dimensions.

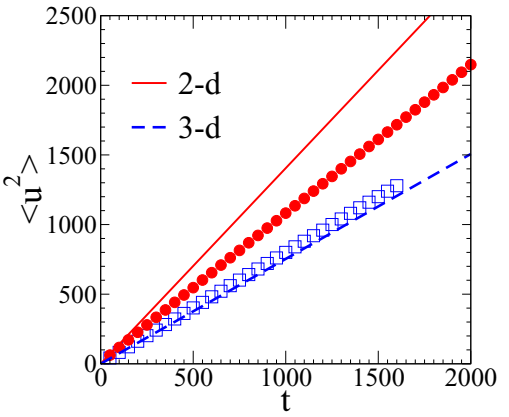

FIG. 3. $\langle u^2 \rangle$ vs. t in two dimensions (solid circles) and three dimensions (open squares) for $\Delta x = 1$. The solid and dashed lines are the Gaussian ansatz predictions for $\langle u^2 \rangle$ in two dimensions and three dimensions, respectively. The uncertainties are smaller than the symbol size.

The extraction of a meaningful value of $u(\vec{r},t)$ in this paper was only possible by rewriting TDGL equation in terms of the deviation of $\psi(\vec{r},t)$ from the bulk equilibrium values and numerically updating this difference [Eq. (10)].

The fact that it is not possible to extract a meaningful auxiliary field from the local state of the system in most models of phase ordering dynamics would seem to call into question whether an analysis based on a Gaussian auxiliary field is be applied in general. However, the closest distance, D, from a point to an interface is well defined in all models of phase ordering systems with scalar order parameter. The equivalence between the auxiliary field u and the closest distance D means that theoretical analysis based on the existence of an auxiliary field is applicable even to the most common case where u cannot be obtained directly from the local order parameter.

Mazenko relates $\langle u(\vec{r},t)^2 \rangle$ to a nonlinear eigenvalue μ with $\langle u^2 \rangle / t = 1.405$ in two dimensions and $\langle u^2 \rangle / t = 0.7534$ in three dimensions [5]. Figure 3 shows that $\langle u^2 \rangle$ obtained from the simulations grows linearly with time as expected. In two dimensions, the slope of 1.081 ± 0.014 is about 20% below the predicted value. One possibility is that this deviation is due to effect of the finite mesh size Δx in the simulations; although universal quantities such as the growth exponent should be independent of the fine details of the model, non-universal quantities such as the growth amplitude may depend on such details. To test for mesh size dependence, I performed simulations in two dimensions with $\Delta x = 0.5$ ($\Delta t = 0.025$) and $\Delta x = 0.25$ ($\Delta t = 0.01$). In both cases the system size was $L_x = L_y = 8192$ and runs were up to $t = 1600$. The slope did not exhibit any systematic dependence on Δx; the slope were 1.094 ± 0.006 and 1.07 ± 0.02 for $\Delta x = 0.5$ and $\Delta x = 0.25$, respectively. Note that the uncertainties for the smaller Δx are very rough estimates based on the variations over five runs each. In three dimensions, the slope of 0.80 ± 0.01 is close to predicted value of 0.7534. The slope of the $\langle u^2 \rangle$ vs. t plots in three dimensions also did not exhibit Δx dependence; the result for $\Delta x = 0.5$ was 0.80 ± 0.02, essentially the same as for $\Delta x = 1.0$.

Figure 4 shows the scaled probability distribution, $L(t)P(u)$, vs. $(u/L(t))^2$ from the two-dimensional simulations. Here, the characteristic length-scale is chosen to be $L(t) = \sqrt{\langle u^2 \rangle}$. The data for the different times show an excellent collapse onto a single master curve as expected from scaling. The data also falls on a straight line on the graph for about five decades in the decay of $P(u)$ indicating that the probability distribution is well approximated as a Gaussian. The only deviation from the Gaussian form occurs near $u/L(t) \approx 0$; the probability distribution becomes flatter than a Gaussian as shown in Fig. 5. This flat region occurs only for $u^2/L(t)^2 < 0.3$ but can be important for the short length and time scale behavior, especially in calculation of the equal time correlation function. On the other hand, the fact that the tails of $P(u)$ are Gaussian would explain why the Gaussian ansatz successfully predicts the decay of the autocorrelation function at large ratio

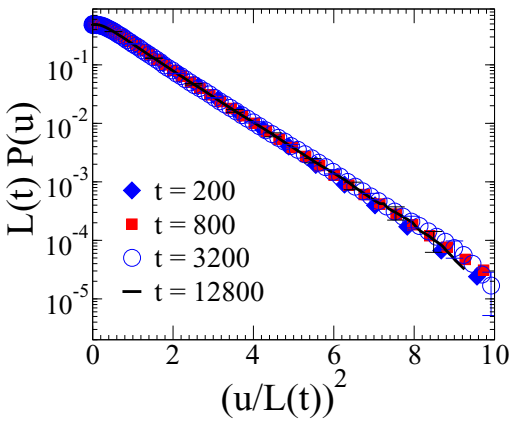

FIG. 4. Semi-log plot of the scaled distribution function $L(t)P(u)$ vs. $(u/L(t))^2$ for four different times in two dimensions. The data shows excellent collapses onto a single scaling curve. The plots all fall on a straight line indicating a Gaussian decay.

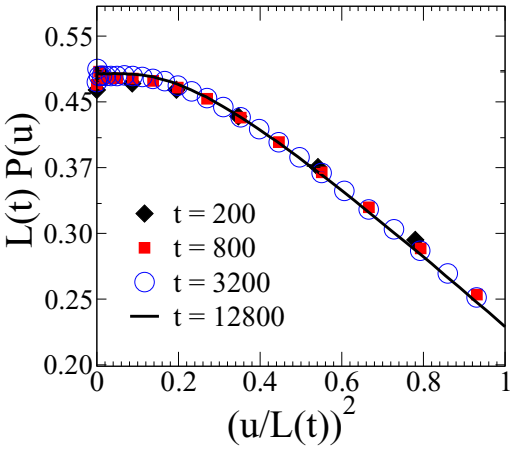

FIG. 5. The same data as in Fig. 4 focusing on small $u/L(t)$. The probability distribution is flatter that that for a Gaussian near $u/L(t) = 0$ but this region is small. Uncertainties are smaller than the symbol size.

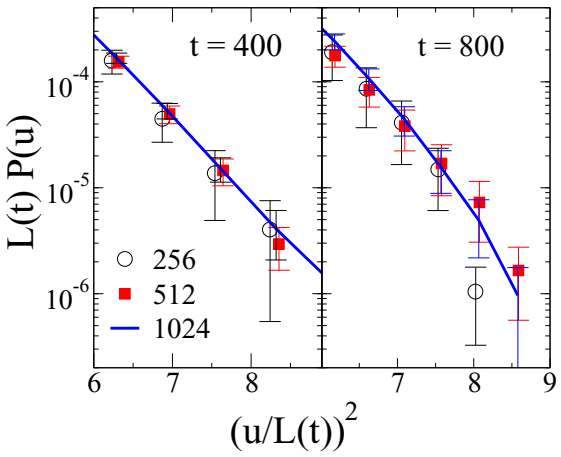

FIG. 7. Test for finite size effects. Scaled distribution function at $t = 400$ and $t = 800$ for 3D systems of size 256^3, 512^3, and 1024^3. No finite size effects are discernible at $t = 400$ but the data for the smaller system size falls off at large u/L at $t = 800$.

of length-scales $L(t)/L(t')$ since the regions of large u will persist in the same order parameter state the longest.

The normalized fourth cumulant, $\tilde{\kappa}_4 = \kappa_4/\kappa_2^2$ is used to quantify how close $P(u)$ approaches a Gaussian. Here κ_4 is the fourth cumulant, and κ_2 is the second cumulant. The value of $\tilde{\kappa}_4$ showed a systematic change from $\tilde{\kappa}_4 \approx -0.35$ at $t = 50$ to $\tilde{\kappa}_4 \approx -0.25$ at $t = 400$. After this transient, there was no systematic change in $\tilde{\kappa}_4$. Averaging over time and initial conditions, I find $\tilde{\kappa}_4 = -0.22 \pm 0.05$. For comparison, $\tilde{\kappa}_4 = 0$ for a Gaussian distribution while $\tilde{\kappa}_4 = +3$ for an exponential distribution, $\tilde{\kappa}_4 = -1.2$ for a uniform distribution, and $\tilde{\kappa}_4 = -2$ for a symmetric two point distribution as would be expected for $P(\psi)$, the distribution of the order parameter. The small value of $\tilde{\kappa}_4$ confirms that the auxiliary field, $u(\vec{r},t)$, is close to a Gaussian random field in two dimensions.

Figure 6 shows the scaled probability distribution, $L(t)P(u)$, from the three-dimensional simulations. Several differences from the two-dimensional case are apparent. First, the curved, non-Gaussian, portion of the graph extends to a much larger range of $u/L(t)$; the curvature in the graph is fairly obvious up to $u^2/L(t)^2 \approx 4$. This is confirmed by the normalized fourth cumulant $\tilde{\kappa}_4 = -0.56 \pm 0.02$, which is more than double the two dimensional case. Secondly, the collapse of the data onto a single master scaling curve is only approximate. At first, it appears that scaling will occur: the scaled distributions for $t = 200$ and $t = 400$ collapses well onto a single curve. Furthermore, the tails of $P(u)$ appears as a straight line on the graph indicating that the distributions at these two times decay as a Gaussian at large $u/L(t)$. However, this does not appear to hold at later times. Instead of reinforcing the curves for $t = 400$ and $t = 800$, the tails of the scaled distribution for $P(u)$ at $t = 800$ and $t = 1600$ show an increasing deviation from the $t = 200$ and $t = 400$ curves.

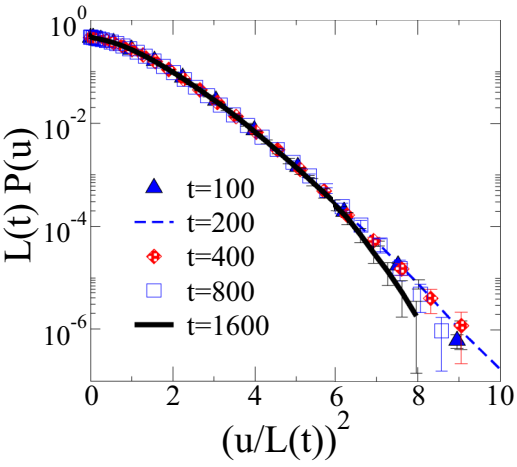

FIG. 6. Semi-log plot of the scaled distribution function $L(t)P(u)$ vs. $(u/L(t))^2$ for five different times for the 3D case. The non-Gaussian region around $u = 0$ extends much further than for the two dimensional case and there is curvature in the tails at late times.

One obvious possibility for the deviation from scaling is that it is due to finite size effects. The system size used for the 3D simulations is only $L_x = 1024$ instead of $L_x = 16384$ used in the two-dimensional simulations. To test for finite size effects, I compare results for systems of size 256^3, 512^3, and 1024^3 at $t = 400$ and at $t = 800$. The data are averaged over 260 initial conditions for the 256^3 simulations and 140 initial conditions for the 512^3 simulations. As shown in Fig. 7, at $t = 400$, the scaled distribution for all three lattices size fall on the same curve, indicating finite size effects are not important at $t = 400$. However, there is discrepancy between the $L_x = 256$ results and the results from the larger lattices at $t = 800$. Assuming that finite size effects depend on the ratio of $L(t)/L_x$, this would imply that finite size effects are unimportant up to $t = 1600$ for $L_x = 512$ and up to $t = 6400$ for $L_x = 1024$. Therefore the change in scaling behavior at late times is most likely not due to finite size effects.

A possible reason for the difference observed in two and three dimensions is that the roughening transition occurs at non-zero temperature in three dimensions [33]. The zero noise TDGL equation is effectively a quench to zero temperature so the interfaces are macroscopically planar for the spatially discretized three dimensional TDGL. This transition from a

smoothly varying to a planar interface at late times may affect the change in scaling behavior observed. Das and Chakraborty also speculated that this transition is also the source of very long transients they observed in quenches of the three-dimensional kinetic Ising model to zero temperature. In particular, they found the characteristic length-scale initially grows as $L(t) \sim t^{1/2}$ but there is then a regime of slower growth until returning to a $t^{1/2}$ asymptotic growth [29,31]. Brown and Rikvold also reported fairly long transients up to $t = 200$ for their 3D integration of the time dependent Ginzburg Landau equation [32]. This long time transient may be reflected in a change in the scaling form of the probability distribution of u.

IV. SUMMARY

The assumption that the order parameter can be mapped to a locally smooth auxiliary field is a useful approach toward a quantitative understanding of non-conserved order parameter phase ordering dynamics. In particular, the ansatz that the auxiliary field is a Gaussian random field leads to predictions of both the equal time correlation function and the decay of the autocorrelation function which are consistent with experiment and simulation. In this paper, I directly test the Gaussian auxiliary field ansatz by numerically integrating the time-dependent Ginzburg-Landau equation and extracting the auxiliary field $u(\vec{r},t)$ from the local order parameter field $\psi(\vec{r},t)$. I also show that the local auxiliary field is equivalent to the distance to the nearest interface. This significant of this equivalence is that it means that approaches using the auxiliary field can be applied even to systems where it is not possible to define this field from the local order parameter.

In two dimensions the probability distribution of $u(\vec{r},t)$ is close to Gaussian except for a small range around $u/L(t) = 0$ which is flatter than a Gaussian distribution. This may account for the small discrepancy between the measured equal time correlation functions and that predicted by the Gaussian ansatz at intermediate values of $r/L(t)$. On the other hand, the predictions using the Gaussian ansatz should work well at large distances or large ratios of times, since these correlations should be determined by regions of large u. which should be dominated by regions with large values of u. In three dimensions, the situation is more complex. The portion of the distribution function around $u/L(t) = 0$, where the distribution is non-Gaussian is much larger than in two dimensions. The tails of the distributions trends toward a Gaussian at intermediate times. However, at later times in this simulation, there appears to be transition to a faster than Gaussian decay.

[1] A. J. Bray, Adv. Phys. **51**, 481 (2002).
[2] S. Puri and V. Wadhawan, *Kinetics of Phase Transitions* (CRC Press, Boca Raton, FL, 2009).
[3] T. Ohta, D. Jasnow, and K. Kawasaki, Phys. Rev. Lett. **49**, 1223 (1982).
[4] Y. Oono and S. Puri, Mod. Phys. Lett. B **2**, 861 (1988).
[5] G. F. Mazenko, Phys. Rev. B **42**, 4487 (1990).
[6] F. Liu and G. F. Mazenko, Phys. Rev. B **44**, 9185 (1991).
[7] F. Liu and G. F. Mazenko, Phys. Rev. B **45**, 4656 (1992).
[8] A. J. Bray and K. Humayun, Phys. Rev. E **48**, R1609 (1993).
[9] C. Yeung, Y. Oono, and A. Shinozaki, Phys. Rev. E **49**, 2693 (1994).
[10] S. M. Allen and J. W. Cahn, Acta Metall. **27**, 1085 (1979).
[11] C. Yeung and D. Jasnow, Phys. Rev. B **42**, 10523 (1990).
[12] F. Liu and G. F. Mazenko, Phys. Rev. B **45**, 6989 (1992).
[13] A. J. Bray and K. Humayun, J. Phys. A: Math. Gen. **25**, 2191 (1992).
[14] M. Rivera, X. L. Wu, and C. Yeung, Phys. Rev. Lett. **87**, 044501 (2001).
[15] K. Humayun and A. J. Bray, Phys. Rev. B **46**, 10594 (1992).
[16] G. Brown, P. A. Rikvold, and M. Grant, Phys. Rev. E **58**, 5501 (1998).
[17] D. S. Fisher and D. A. Huse, Phys. Rev. B **38**, 373 (1988).
[18] K. Humayun and A. J. Bray, J. Phys. A **24**, 1915 (1991).
[19] N. Mason, A. N. Pargellis, and B. Yurke, Phys. Rev. Lett. **70**, 190 (1993).
[20] A. J. Bray and B. Derrida, Phys. Rev. E **51**, R1633 (1995).
[21] C. Yeung, M. Rao, and R. C. Desai, Phys. Rev. E **53**, 3073 (1996).
[22] G. F. Mazenko, Phys. Rev. E **69**, 016114 (2004).
[23] M. Henkel, A. Picone, and M. Pleimling, Europhys. Lett. **68**, 191 (2004).
[24] F. Corberi, E. Lippiello, and M. Zannetti, Phys. Rev. E **72**, 056103 (2005).
[25] M. Henkel and F. Baumann, J. Stat. Mech.: Theory and Experiment (2007) P07015.
[26] F. Baumann and M. Pleimling, Phys. Rev. B **76**, 104422 (2007).
[27] J. Midya, S. Majumder, and S. K. Das, J. Condens. Matter **26**, 452202 (2014).
[28] T. Blanchard, L. F. Cugliandolo, and M. Picco, J. Stat. Mech.: Theory Exp. (2014) P12021.
[29] S. Chakraborty and S. K. Das, Eur. Phys. J. B **88**, 160 (2015).
[30] F. Corberi and R. Villavicencio-Sanchez, Phys. Rev. E **93**, 052105 (2016).
[31] S. K. Das and S. Chakraborty, J. Eur. Phys. J. Spec. Top. **226**, 765 (2017).
[32] G. Brown and P. A. Rikvold, Phys. Rev. E **65**, 036137 (2002).
[33] S. T. Chui and J. D. Weeks, Phys. Rev. B **14**, 4978 (1976).